A long waves propagation in two-layer fluid over a circular bowl pit

Fatimah Noor Harun'

Citation: AIP Conference Proceedings **1750**, 030009 (2016); doi: 10.1063/1.4954545
View online: http://dx.doi.org/10.1063/1.4954545
View Table of Contents: http://aip.scitation.org/toc/apc/1750/1
Published by the American Institute of Physics

A Long Waves Propagation in Two-Layer Fluid over a Circular Bowl Pit

Fatimah Noor Harun[1,a)]

[1]*School of Informatics and Applied Mathematics,*
Universiti Malaysia Terengganu, 21030 Kuala Terengganu, Terengganu

[a)] Corresponding author: fnoor_hh@umt.edu.my

Abstract. This study is conducted to study the long wave propagation in two layer fluid model over a circular bowl pit by using the analytical solution. The equation used in this study is the mild-slope equation and linear shallow water equation. The methods used to solve this problem are separation of variable and Frobenius series. The mild-slope equation used in this research is a power fool tool to study wave refraction and diffraction over the circular bowl pit in a constant depth region. As part of verification process, this solution is reduced to one-layer fluid and find that our solution agree well with the existing solution. After solving this problem analytically, we find that the depth and the radius of bowl fit have significance effect to the surface wave elevation, η. Besides, the density ratio also give significance effect to the surface wave elevation.

INTRODUCTION

From the observation about ocean waves from the surface, the phenomenon such as shaking ships during storms in the open ocean, or breaking rhythmically near the shore are usually seen. However, much of the ocean wave action takes place underneath the surface, and consists of modulations not of the air–water interface, but of invisible surfaces of constant density, which known as internal waves. These *internal waves* are ubiquitous in the ocean, contain a large amount of energy, and affect significantly the processes involved in water mixing and transport[1].

Internal waves have become popular among the researchers since Ekman's theoretical explanation of "dead water" experience by slowly-moving vessels [2]. The propagation of waves in a two-layer fluid with both a free surface and an interface (in the absence of any obstacles) was first investigated by Stokes [3]and a description of some of the types of wave motion which can occur is given by Lamb [4]. Replacing the free surface with a rigid-lid approximation is reasonable in many cases, especially at the regional ocean scale, because "internal-wave mode" only induces small deformation on the free surface and thus a rigid-lid approximation would exclude the fast mode associated with barotropic free surface waves and greatly simplify the theoretical analysis without loss of a great deal of accuracy. Much work also has been done on internal solitary waves in two-layer fluids, pioneered by authors such as Keulegan [5], Long [6], and Benjamin [7]. However, until recently, very little work has been done on wave/structure interactions in two-layer fluids.

Recently, by utilizing the modified mild-slope equation constructed previously by Chamberlain and Porter [8], Chamberlain and Porter [9]then derived a mild-slope equation for a two-layer fluid model. Their results is capable for accurately calculating wave scattering induced by singly and doubly periodic ripple beds, for which the Berkhoff's mild-slope equation fails. More recently, Zhu and Harun [10], constructed the two-layer mild-slope equation with the rigid lid approximation is used for the upper-layer. Based on the equation obtained, they then derived the analytical solution for long waves propagating over a circular hump located at the bottom of a two-layer ocean.

In this paper, utilizing the work done by Zhu and Harun[10], an analytical solution for long waves propagating over a circular bowl-pit located at the bottom of a two-layer ocean is derived. Then, as a verification processes, the new analytic solution in a special case of the two-layer fluid model, i.e $\rho_1 = 0$ with the solution in single-layer fluid

Advances in Industrial and Applied Mathematics
AIP Conf. Proc. 1750, 030009-1–030009-10; doi: 10.1063/1.4954545
Published by AIP Publishing. 978-0-7354-1407-5/$30.00

model obtained by Suh et. al [11]are compared. Using the new solution, the effects of the pit dimensions on the wave refraction are discussed. Finally, the main findings in this paper are briefly summarized in the last section.

ANALYTIC SOLUTION

In this section, by utilizing Harun's [12]derivation for mild-slope equation in a two-layer fluid model, the analytic solution for long waves propagating in a two-layer fluid over a circular bowl pit are presented.

Long Waves Propagating over a Circular Bowl-pit

Consider a train of plane long waves which propagates in two-layer fuids with constant water depth h_1 and h_{20}, densities of lower and upper layer ρ_1 and ρ_2 and is refracted by an axi-symmetric bowl-pit located on the ocean floor as shown in Figure 1.

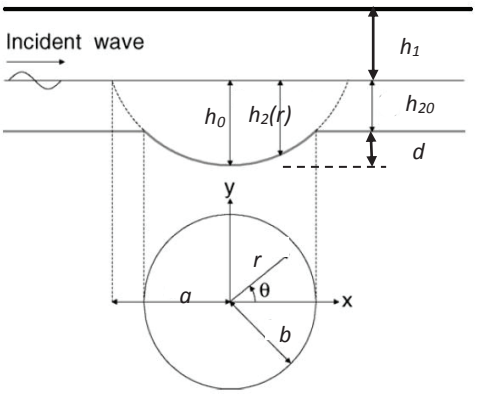

FIGURE 1. A definition sketch of a bowl-pit located on the floor in two-layer fluid system.

The cross-section of the bowl-pit is of the shape of a parabola and decreases gradually from the center to the edge, resulting in a circle with its radius denoted as b, and a is the radial distance from the pit center to the imaginary edge of the pit extended to the water surface. The height of the hump is controlled by a parameter d as shown in Figure 1. In the corresponding cylindrical coordinate system with r being the radial distance from the origin and θ being the angle measured counterclockwise from the positive x axis, the water depth for the lower layer is prescribed by a parabolic function

$$h_2(r) = \begin{cases} (h_{20}+d)\left(1-\dfrac{r^2}{a^2}\right), & r < b \\ (h_{20}+d)\left(1-\dfrac{b^2}{a^2}\right), & r \geq b \end{cases} \tag{1}$$

The mild slope wave equation is given by

$$\nabla.\left(CC_g\nabla\eta\right) + k^2 CC_g\eta = 0\,, \tag{2}$$

where η, C, C_g, k and ∇ are the complex water surface elevation, the phase speed, the group velocity, the wave number, and the horizontal gradient operator respectively. When the wavelength is much longer than the wave height, Eq. (2) can be reduced to a long (shallow water) wave equation which takes the form

$$\nabla.\left(\frac{(\rho_2-\rho_1)h_1h_2}{\rho_1h_2+\rho_2h_1}\nabla\eta\right) + \frac{\sigma^2}{g}\eta = 0, \tag{3}$$

under the assumption $C \cong C_g \cong \sqrt{\frac{g(\rho_2-\rho_1)h_1h_2}{\rho_1h_2+\rho_2h_1}}$ and $\sigma^2 \cong \frac{gk^2(\rho_2-\rho_1)h_1h_2}{\rho_1h_2+\rho_2h_1}$, where g is the gravitational acceleration, σ is the angular velocity, h_1 and h_2 are the local water depth for the upper and lower layer respectively.

We shall now present an exact solution following Zhu and Harun [10], Zhang and Zhu[13], and Suh et. al. [12] approached for their solution of progressive waves on the free surface of a single layer of fluid over an axi-symmetric shaped located on the ocean floor.

It is convenient to adopt a cylindrical coordinate system (r, θ, z) with $x = r\cos(\theta)$ and $y = r\sin(\theta)$, because the bottom topography of this problem is axi-symmetric with respect to the z-axis. Thus, Eq. (3) can be written as

$$r^2\frac{\partial^2\eta}{\partial \mathrm{r}^2} + r\left(1+\frac{r}{h}\frac{\partial h}{\partial \mathrm{r}}\right)\frac{\partial\eta}{\partial \mathrm{r}} + \frac{\partial^2\eta}{\partial\theta^2} + \frac{\mu r^2}{\mathrm{h}}\eta = 0\,, \tag{4}$$

where $h = \frac{(\rho_2-\rho_1)h_1h_2}{\rho_1h_2+\rho_2h_1}$ and $\mu = \frac{\sigma^2}{g}$. The method of separation of variables can be used because, $h_2(r)$ is a function of r only. Thus, let

$$\eta(r,\theta) = \sum_{n=0}^{\infty} R_n(r)\cos(n\theta), \tag{5}$$

with R_n satisfying

$$(\rho_1h_2+\rho_2h_1)(a^2-r^2)r^2\frac{d^2R_n}{dr^2} + ((\rho_1h_2+\rho_2h_1)(a^2-r^2)r) - 2r^2\rho_2h_1\,r^3)\frac{dR_n}{dr} + \left(\frac{(\rho_1h_2+\rho_2h_1)^2}{(\rho_2-\rho_1)h_1}v^2r^2 - n^2(\rho_1h_2+\rho_2h_1)\,(a^2-r^2)\right)R_n = 0\,, \tag{6}$$

where $v = \frac{\sigma a}{\sqrt{gh_{20}}}$.

The general solution for Eq. (6) can be obtained in terms of Frobenius Series[14]:

$$R_n(r) = \sum_{m=0}^{\infty}\alpha_{m,n}r^{m+c},, \tag{7}$$

with $\alpha_{0,n} = 1$ and c being a constant to be determined by the indicial equation.

It should be emphasized that convergence of the series solution is guaranteed at $r < a$. Therefore, the solution always converges in the pit region with $r < b$. Solving Eq. (6) using the Frobenius series, the indicial equation, $c^2 - n^2 = 0$ is obtained; which yields two roots, $c = \pm n$. These two distinct roots of the indicial equation lead to two sets of linearly independent solutions:

$$R_{n,1} = \sum_{m=0}^{\infty}\alpha_m r^{m+n}, \tag{8}$$

$$R_{n,2} = R_{n,1}\ln(r) + \beta_{m,n}r^{m-n}\,. \tag{9}$$

Since $R_{n,2}$ becomes singular at $r = 0$, it has to be discarded, with the imposition of the condition that water surface elevation must be finite at the origin.

Now, substituting Eq. (8) into Eq. (6) and collecting the terms of the same order of r, we obtain

$$\alpha_{1,n} = \alpha_{3,n} = \alpha_{5,n} = 0\,, \tag{10}$$

$$\alpha_{2,n} = \frac{-\left\{2Bn - \frac{v^2F^2}{D}(A+B)^2\right\}\alpha_{0,n}}{4a^2F\{1+n\}}\,, \tag{11}$$

$$\alpha_{4,n} = \frac{\left\{4[2A+B]+4[(2A+B)n-B]-2Bn-\frac{v^2F^2}{D}\right\}\alpha_{2,n} + \left\{\frac{2v^2EF}{D}\right\}\alpha_{0,n}}{8a^2F(2+n)}, \tag{12}$$

$$\alpha_{m,n} = \frac{\{(m-2)^2\gamma_2+2(m+2)[\gamma_2 n-B]-2Bn-\gamma_3\}\alpha_{m-2,n} - \{E[(m-4)((m-4)+2n)]-\gamma_1\}\alpha_{m-4,n}-\gamma_4\,\alpha_{m-6,n}}{a^2Fm\,(m+2n)}, \tag{13}$$

with m =6,7,8,…, and $A = \rho_1(h_{20}), B = \rho_2 h_1, D = (\rho_2 - \rho_1)h_1$, $E = \frac{A}{a^2}, F = \frac{A}{D}$, $\gamma_1 = \frac{2v^2F}{D}$, $\gamma_2 = 2A + B, \gamma_3 = \frac{v^2F^2}{D}, \gamma_4 = \frac{v^2E^2}{D}$.

Where m denotes the number of recurrence solutions for Frobenius series solution that we have to find until our solution is converged to a desire point, while n corresponds to the wave propagation modes.

For the general solution in the finite region with variable depth $r < b$, the water surface elevation can be written as:

$$\eta_2 = \sum_{n=0}^{\infty} B_n R_n cos\, n\theta, \tag{14}$$

where B_n is a set of complex constants to be determined by matching the solution in this region with that in the region of constant water depth. The undisturbed long-crested incident waves propagate in the positive x-direction and its surface elevation is given by Mei [15]:

$$\eta_0 = a_i e^{ikx} = a_i \sum_{n=0}^{\infty} i^n \varepsilon_n J_n(kr)\cos(n\theta), \tag{15}$$

where a_i is the incident wave amplitude and $i = \sqrt{1}$, J_n is the Bessel function of the first kind of order n, and ε_n is the Jacobi symbol defined by

$$\varepsilon_n = \begin{cases} 1, & n = 0, \\ 2, & n \geq 1. \end{cases} \tag{16}$$

In the constant depth region ($r > b$), the solution is well known as given in MacCamy and Fuch [16]:

$$\eta_1 = \eta_0 + \sum_{n=0}^{\infty} D_n H_n^{(1)}(kr) cos\, n\theta, r \geq b, \tag{17}$$

where D_n is some unknown coeffcients to be determined later, and $H^{(1)}_n$ is the Hankel function of the first kind of order n.

The solutions in these two sub-regions must be matched on the common boundary $r = b$ to ensure the continuity of wave heights and the hydrodynamic pressure across it [17]. Thus, it requires that

$$\eta_1 = \eta_2 \text{ at } r = b, \tag{18}$$

$$\frac{\partial \eta_1}{\partial r} = \frac{\partial \eta_2}{\partial r} \text{ at } r = b. \tag{19}$$

Therefore, from Eqs. (18)-(19), the coeffcients B_n and D_n can be determined as

$$B_n = k a_i i^n \varepsilon_n \frac{J_n(kb)H_n^{(1)\prime}(kb) - J'_n(kb)H_n^{(1)}(kb)}{kR_n(b)H_n^{(1)\prime}(kb) - R'_n(b)H_n^{(1)}(kb)}, \tag{20}$$

$$D_n = a_i i^n \varepsilon_n \frac{kJ\prime_n(kb)R_n(b) - J_n(kb)R\prime_n(b)}{H_n^{(1)}(kb)R\prime_n(b) - kH_n^{(1)\prime}(kb)R_n(b)}. \tag{21}$$

in which the primes denote the derivatives with respect to the argument. By substituting these coeffcients back into Eqs. (14) and (17), the water surface elevation for the entire domain can be computed. Some results of specific calculations are presented in the next section.

RESULTS AND DISCUSSIONS

The results of the analytic solution for wave propagating in two-layer fluid over a circular bowl-pit will be presented and discussed in this sections. Firstly, we will compare our solution with the special case presented by Suh et. al [11]. Then, we examine the effect of wave refraction when the ratio of the densities, ρ_1/ρ_2 and the ratio of upper and lower water depth, h_1/h_2 are varied. Lastly, using the new solution, we discuss the effect of pit dimensions on the wave refraction process over a bowl-pit.

Comparison with the Single Fluid Model

If we set ρ_1=0, the mild-slope equation for a two-layer fluid model should reduce to a single-layer model, thus, it would be interesting to compare both models, as part of the verification process. We take $\rho_1 = 0$, $\rho_2 = 5$, $h_1 = h_2 = 4.8$, and set the remaining parameters exactly the same as those used in single-layer fluid model discussed in Suh et.al [11], i.e, $b/L = 0.5$, and the wave length, $L = 120.4$. Since, the analytic solution for η involves an infinite series, it must be truncated for the purpose of numerical solution, so we set $N = 70$ and $M = 30$, because the solution had already converged with these values. The Bessel and Hankel functions in the analytical solution were computed using the built-in subroutines in MATLAB.

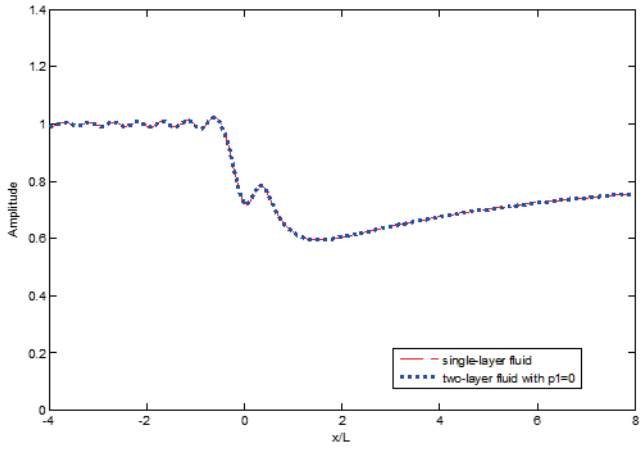

FIGURE 2. The relative wave amplitude along the x- axis for the two- and single-layer fluid models

Figure 2 shows the comparison of the relative wave amplitude along the x- axis for the two- and single-layer fluid models. The result in this comparison are presented in terms of dimensionless coordinates, $x=L$ and the centers of the pit is located at the origin. As expected, the results are reasonably close each other. With the excellent agreement between these solutions, we are confident that the derivation of our new analytical solution is correct.

Next, the contour plots of the relative wave amplitudes (i.e. the wave amplitude relative to the incident amplitude) for long waves propagating over the circular bowl pit in two layer fluid is presented in Figure 3. The results are presented in terms of dimensionless coordinates, x/L and y/L. The centers of the pit is located at the origin and the contour lines in the each plot show the values of the relative wave amplitude. From this plot, we can see that the incoming wave begin to refract the bowl-pit area. When entering the pit area, the relative wave sligtly increase before begin to reduce in the shadow zone. The discussion about the effect of the density, water depth and pit profile will be presented in the next section.

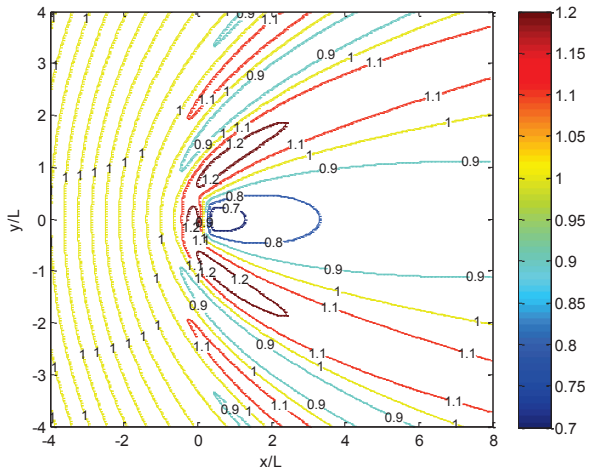

FIGURE 3. Contour plots of the relative wave amplitudes

Effect of the Density Ratio

In this section, the effect of the wave refraction when the ratio of the densities, ρ_1/ρ_2 is varied is discussed, while other parameters are held constant. In order to examine this, let ρ_1/ρ_2 = 1/5, 2/5, 3/5, and 4/5 with the pit radius being fixed at b/L = 0.5 and $h_1 = h_2 = 4.8$ are used.

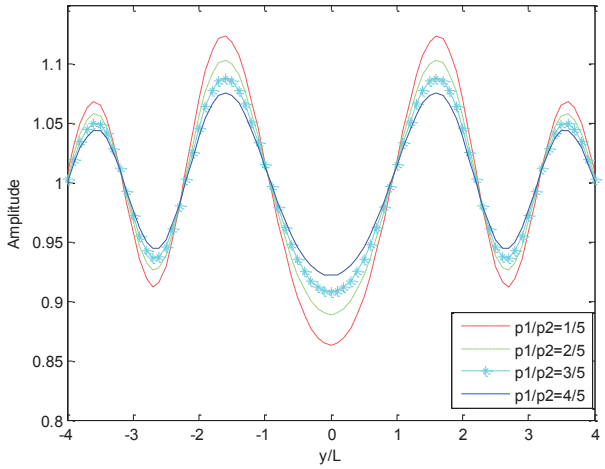

FIGURE 4. Comparisons for each value of ρ_1/ρ_2 along the x-axis

Figure 4 and Figure 5 show the comparisons for each value of ρ_1/ρ_2 along the x- and y-axes respectively. As expected, an increase in the ratio of the densities, ρ_1/ρ_2 results in the smaller relative wave amplitudes. As shown in both figures, when ρ_1/ρ_2=1/5, the relative wave amplitude is bigger than when ρ_1/ρ_2=4/5. It is because, when ρ_1/ρ_2=4/5 there is a smaller density difference between the two layers, resulting in a weaker restoring force for both layers [10].

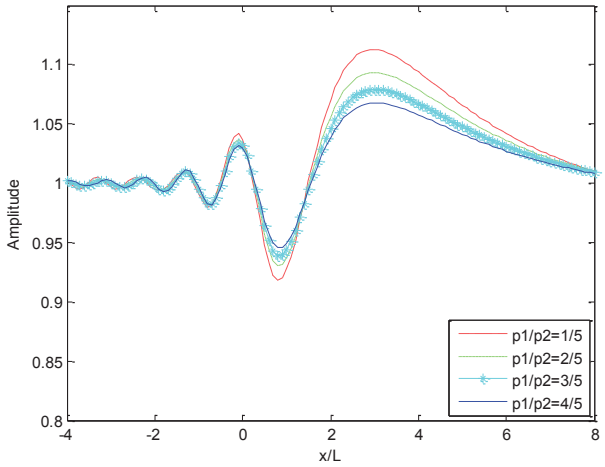

FIGURE 5. Comparisons for each value of ρ_1/ρ_2 along the y-axis

Effect of the Layer Thickness

Next, we study the effect of the wave refraction when the ratio of the upper and lower water depth, h_1/h_2 is varied, while the total water depth and other parameters remain unchanged. Figures 6 and 7 illustrate the relative wave amplitude for three different values of h_1/h_2, i.e h_1/h_2=1/2, h_1/h_2=1 and h_1/h_2=2, with ρ_1/ρ_2 = 3/5 along the x- and y-axes to examine the effects of the layer thickness to the wave refraction. Here, we set the others parameters as before and only vary the upper and lower water depth in such a way that the total water depth is kept the same.

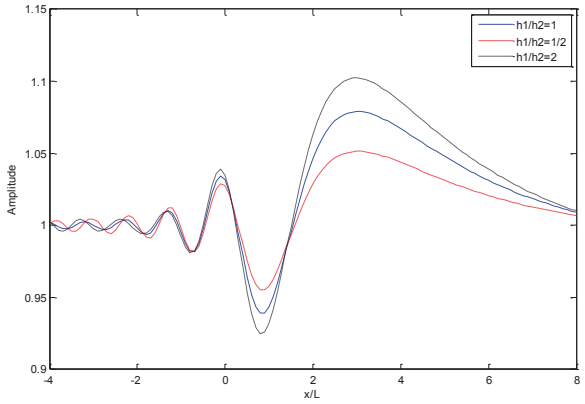

FIGURE 6. Comparisons for each value of h_1/h_2 along the x-axis

As shown in both figures, when the lower layer has less fluid than the upper layer, i.e $h_1/h_2 = 2.0$, the relative wave amplitude has been amplified more. This phenomenon occurs because, when the upper layer is thicker than the lower layer, the incident waves can "feel" the bottom topography more, as the interface is closer to the seabed. Therefore, the interfacial waves can refract more, resulting in a bigger relative wave amplitude. In contrast, when there is more fluid in lower layer, i.e $h_1/h_2 = 1/2$, there is more fluid in lower layer, and thus the influence of seabed is less, resulting in the smaller relative wave amplitude [10].

Topographic Effect

Next, the effects of the wave refraction when the dimension of the bottom topography is varied is examined. In Figs. 8 and 9 we plot the relative wave amplitudes along the x- and y-axes for different pit radii, $b/L = 0.25$, 0.5, 0.75 and 1.0 with a fixed $d = 0.5$ and $h_2 = 4.8$ with $\rho_1/\rho_2 = 3/5$, respectively.

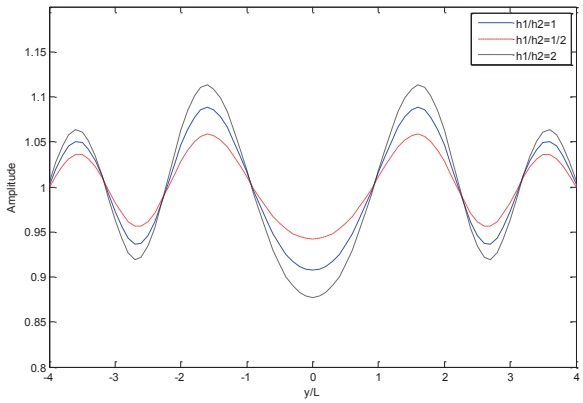

FIGURE 7. Comparisons for each value of h_1/h_2 along the y-axis

Along the x- and y-axes, the relative wave amplitude in front of the pit increases with the increase of the pit radius. However, as can be seen in Figure 8, in the shadow zone (after the pit area) the increase of the pit radius resulting in the bigger wave reduction. It is because as the pit radius increase with respect to the maximum depth, the slopes within the pit decrease, hence less wave reflection occurs.

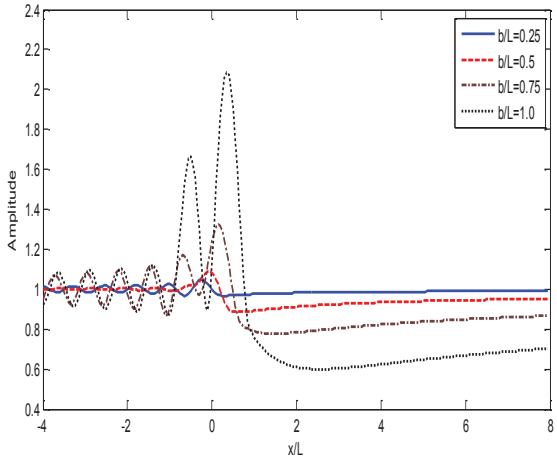

FIGURE 8. Comparisons for each value of pit radius, b/L along the x-axis

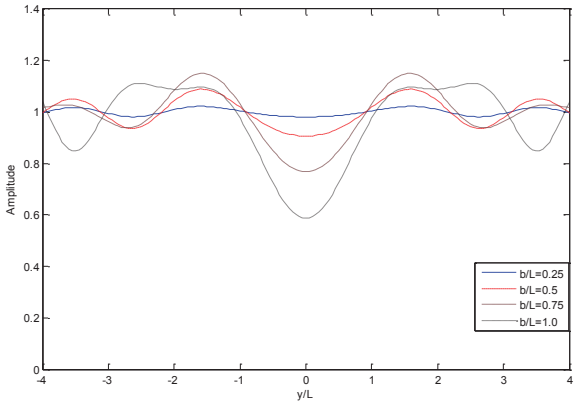

FIGURE 9. Comparisons for each value of pit radius, b/L along the y-axis

Then, the effects of the wave refraction when the depth of the pit, d is varied is discussed. Figure 10 and Figure 11 show the relative wave amplitude along the x- and y- axes, respectively, for the cases of d = 0.5, 1.0, 1.5, and 2.0 with the pit radius being fixed at b/L = 0.5, ρ_1/ρ_2 = 3/5, and h_1/h_2= 4.8. As can be clearly seen from both figures, as expected, the deeper the pit is, the more intensified fluctuation the wave refraction causes.

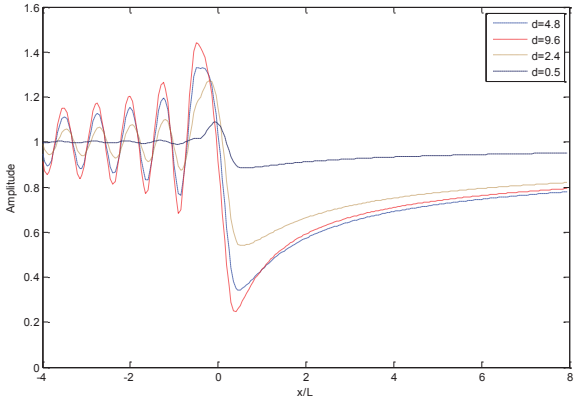

FIGURE 10. Comparisons for each value of pit depth, d along the x-axis

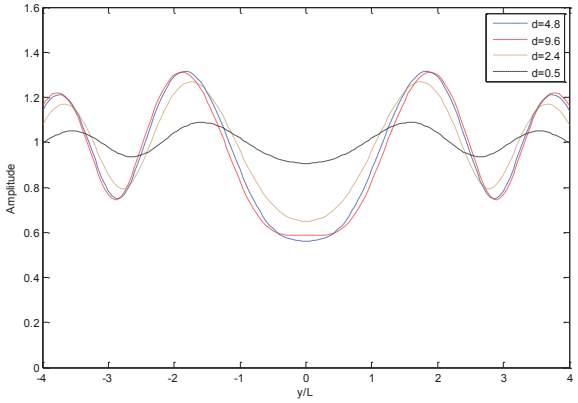

FIGURE 11. Comparisons for each value of pit depth, d along the y-axis

For a pit with a shallower depth, d=0.5, the refraction effects are weak, resulting in an almost even distribution of wave heights across the pit. As the depth of the pit increases, the partial standing wave in front of the pit also increases, resulting in more wave energy scattered laterally due to refraction. Thus, as can be seen in Figure 10, the wave amplitude will decrease in the shadow zone.

CONCLUSIONS

We have derived analytical solution for wave propagating for a two-layer fluid model with the rigid-lid approximation used on the free surface propagating over a circular bowl-pit. This analytic solution was derived based on the two-layer mild-slope equation obtained by Zhu and Harun [10] and verified it with the analytical solution for wave propagating in a single-layer fluid model over a circular bowl-pit by Suh et. al [11] because the single-layer model is the special case for a two-layer model when the density of the upper layer, ρ_1 equal to zero. We then made a comparison for both solutions, by letting ρ_1=0 for the two-layer fluid equation, and found that the two solutions were identical and hardly distinguishable, as expected.

Furthermore, we have also examined and discussed the effects of the wave refraction when the ratio of densities, ρ_1/ρ_2 and the ratio of the upper and lower layer water depths, h_1/h_2 are varied. When the ratio of the densities, ρ_1/ρ_2 is increased, the relative wave amplitude decreases. This is because, when ρ_1/ρ_2 increases, the density difference between each layer became smaller, resulting in a weaker restoring force. Thus, the weaker restoring force induces a smaller relative wave amplitude. For the test of the h_1/h_2 , the relative wave amplitude increases with the increasing of h_1/h_2 .

Finally, we have also observed and discussed the effect of the pit dimension when the radius, b/L and the depth of the pit, d are varied. Here, we found that an increase in the radius and the height of the hump led to a reduction of the relative wave amplitude in the shadow area.

ACKNOWLEDGMENTS

The authors acknowledge the financial and facilities support from RAGS grant (Vot No: 57105) from Ministry of Higher Education (MOHE), and School of Informatics and Applied Mathematics, Universiti Malaysia Terengganu, Kuala Terengganu, Terengganu, Malaysia.

REFERENCES

1. Y. Lvov and E. G. Tabak, Physica D **195**. 106-122(2004).
2. V. W. Ekman, Scientific Results of the Norwegian North Polar Expedition 1893-1896, 5(15), 1904.
3. G. G. StokesTrans. Camb. Phil. Soc. **8**. 441-455 (1847).
4. H. Lamb, *Hydrodynamic*, sixth ed., (Cambridge University Press, 1932).
5. G. H Keulegan, J. Res. Natl. Bur. Stand **51**. 133.1953.
6. R. R. Long, Tellus **8**, 460.1956.

7. T. B. Benjamin, J. Fluid Mech **146**, 559-592.1967.
8. P. G. Chamberlain and D. Porter, J. Fluid Mech. **291.** 393-407.1995.
9. P. G. Chamberlain and D. Porter,J. Fluid Mech. **524.** 207-228. 2005.
10. S.P-.Zhu and F. N. Harun, Journal of Applied Mathematics and Computing, **30** (1-2). 315-333.2009.
11. K.D. Suh, T.-H. Jung, and M.C. Haller, Wave Motion **42**, 143-154.2005.
12. F. N. Harun "Analytic solutions for linear waves propagating in an ocean with variable bottom topography and their applications in renewable wave energy", PhD Thesis, University of Wollongong, 2009.
13. Y. Zhang and S.-P. Zhu. J. Fluid Mech. **278.**391-406.1994.
14. F.B. Hildebrand. *Advanced Calculus for Applications* (Prentice-Hall, Englewood Cliff, New Jersey, second edition, 1976).
15. C.C. Mei. *The Applied Dynamics of Ocean Surface Waves* (World Scientific, Singapore, 1989).
16. R.C. MacCamy and R.A. Fuchs. US Army Corps of Engineering, Beach erosion Board, Washington DC, Technical Memorandum, 69, 1954.
17. R.G. Dean and R.A. Dalrymble. *Water Wave Mechanics for Engineers and Scientists* (World Scientific, 1991).